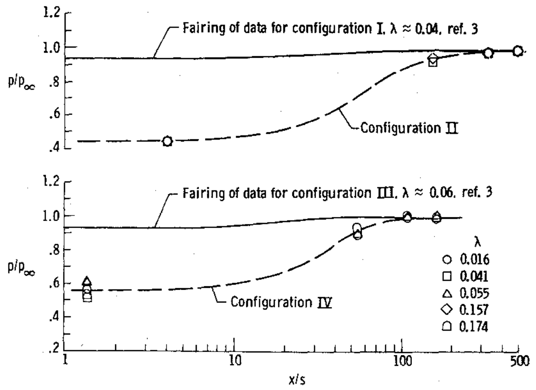

Fig. 1 Surface static pressures downstream of slot configurations.

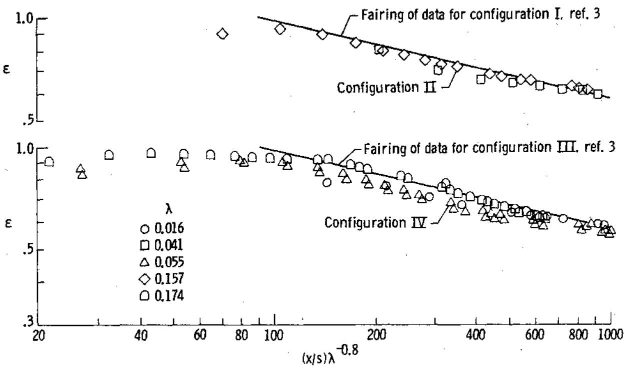

Fig. 2 Film cooling effectiveness for thick slot lip (configuration II) and elevated injection slot (configuration IV).

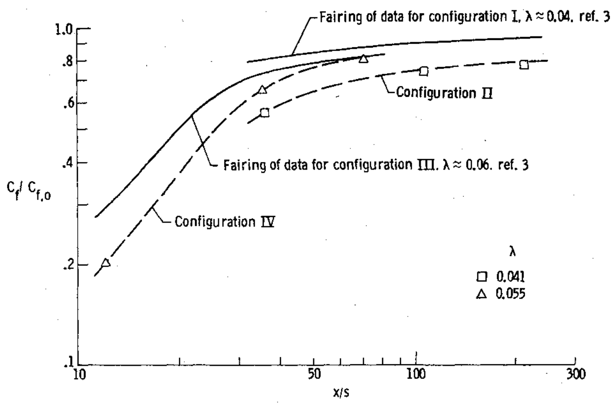

Fig. 3 Skin friction reduction for slot injection configurations.

found previously for the "baseline" slot configurations. Although it was intended to simply show the influence of the thick slot lip or the elevated slot, these data also include the influence of an overall increase in step height.

The effect of the slot modifications on the downstream skin friction is shown in Fig. 3 for slot mass flow ratios comparable to the nearly "matched" pressure conditions found for the "baseline" configurations. Configurations II and IV produced significantly larger local and integrated skin friction reductions in comparison to the "baseline" configurations. In fact, configuration II reduced the integrated skin friction over a distance of x/s between 36 and 210 by 15% below that obtained for configuration I; configuration IV produced an additional 5% skin friction reduction over that obtained for configuration III between x/s of 12 and 70. The reduced skin friction may be attributed to the larger step heights and rather severe adverse pressure gradients created by the modified slot configurations.

Although the present results show that simple modifications to the "baseline" slot configurations can enhance the skin friction reductions obtained with tangential slot injection, slot base drag estimates indicate that neither of the modifications will lessen the impact of the systems penalties for collecting, ducting, and injecting the slot air. The base drag for configuration II with the thick slot lip is over eight times greater than the incremental skin friction reduction obtained with that configuration; the base drag for configuration IV with the elevated slot is approximately fifteen times greater than the incremental skin friction reduction obtained with that configuration. Therefore, both of the present modified slot configurations significantly increase the overall slot-injection systems penalties.

References

[1] Parthasarathy, K. and Zakkay, V., "An Experimental Investigation of Turbulent Slot Injection at Mach 6," *AIAA Journal*, Vol. 8, July 1970, pp. 1302-1307.

[2] Cary, A. M. Jr. and Hefner, J. N., "Film Cooling Effectiveness in Hypersonic Turbulent Flow," *AIAA Journal*, Vol. 8, Nov. 1970, pp. 2090-2091.

[3] Cary, A. M. Jr. and Hefner, J. N., "Film Cooling Effectiveness and Skin Friction in Hypersonic Turbulent Flow," *AIAA Journal*, Vol. 10, Sep. 1972, pp. 1188-1193.

[4] Marino, A., Economos, C., and Howard, F. G., "Evaluation of Viscous Drag Reduction Schemes for Subsonic Transports," NASA CR-132718, Nov. 1975.

[5] Goldberg, T. J. and Hefner, J. N., "Starting Phenomena for Hypersonic Inlets with Thick Turbulent Boundary Layers at Mach 6, NASA TN D-6280, Aug. 1971.

[6] Hefner, J. N., Cary, A. M. Jr., and Bushnell, D. M., "Investigation of the Three-Dimensional Turbulent Flow Downstream of Swept Slot Injection in Hypersonic Flow," AIAA Paper 74-679 and ASME Paper 74-HT-13, Boston, Mass., 1975.

On Thermally Induced Non-Fourier Stress Waves in a Semi-Infinite Medium

Tsai-Tse Kao*
Foster Wheeler Energy Corp., Livingston, N.J.

Nomenclature

c = velocity of thermal wave
c_v = specific heat
c_e = stress wave velocity
k = thermal conductivity
I_0 = Bessel function of order zero
I_1 = Bessel function of order one
t = time
T = temperature
$\bar{T}$ = Laplace transform of T with respect to time variable
T_0 = reference temperature
p = Laplace transform variable
q = heat flux
u = elastic displacement
x = space variable
α = thermal diffusivity
$\tilde{\alpha}$ = thermal expansion coefficient
ρ = density
λ,μ = Lame's constants
σ_{xx} = stress in x-direction
$\bar{\sigma}$ = Laplace transform of σ

Received Sept. 22, 1975; revision received Feb. 23, 1976.
Index category: Thermal Stresses; Heat Conduction.
*Sr. Thermal/Hydraulic Engineer, Nuclear Department.

Introduction

THIS brief note investigates analytically the non-Fourier effect of a thermally induced stress wave, using the relaxation heat conduction equation

$$\frac{1}{C^2}\frac{\partial^2 T}{\partial t^2}+\frac{1}{\alpha}\frac{\partial T}{\partial t}=\nabla^2 T$$

where C is the speed of heat propagation. Boley[1] pointed out that for most practical conduction problems, this effect of finite heat propagation speed is negligible. However, as shown in Refs. 2, 3 and 4, this finite speed of heat propagation can become important at very low temperature, or when the elapsed time during a transient is small. Recently, Maurer and Thompson[5] demonstrated that this relaxation heat conduction model predicts an instantaneous jump in the surface temperature of a semi-infinite medium, subjected to a step change in surface heat flux, as opposed to a smooth rise in surface temperature predicted by the conventional Fourier heat conduction model. Thus under sufficiently high flux conditions, this jump in surface temperature may result in very severe thermal stress at the surface. This technical note investigates the effect of this finite heat propagation speed on a thermally induced stress wave in a one-dimensional half-space.

Analysis

Consider a semi-infinite elastic medium with uniform temperature distribution initially, and the intial heat flux is zero, which is equivalent to requiring that the initial time rate of change of the temperature be zero. At $t=0$, a constant heat flux of magnitude F_0 is applied to the traction free surface at $x=0$. The general governing one-dimensional thermal elastic equations are:

$$\rho c_v\frac{\partial T}{\partial t}+(3\lambda+2\mu)\tilde{\alpha}T_0\frac{\partial^3 u}{\partial x\partial t^2}=-\frac{\partial q}{\partial x} \tag{1}$$

$$\frac{\alpha}{c^2}\frac{\partial q}{\partial t}+q=-k\frac{\partial T}{\partial x} \tag{2}$$

$$\frac{1}{c_e^2}\frac{\partial^2 u}{\partial t^2}=\frac{\partial^2 u}{\partial x^2}-\frac{(3\lambda+2\mu)\tilde{\alpha}}{(\lambda+2\mu)}\frac{\partial T}{\partial x} \tag{3}$$

where

$$c_e=\sqrt{(\lambda+2\mu)/\rho} \tag{4}$$

Equations (1) and (2) can be combined together to yield the relaxation energy equation:

$$\frac{1}{c^2}\frac{\partial^2 T}{\partial t^2}+\frac{1}{\alpha}\frac{\partial T}{\partial t}+\frac{(3\lambda+2\mu)\tilde{\alpha}T_0}{k}\left\{\frac{\alpha}{c^2}\frac{\partial^3 u}{c\,\partial x\partial t^2}+\frac{\partial^2 u}{\partial x\partial t}\right\}=\frac{\partial^2 T}{\partial x^2} \tag{5}$$

For the problem under consideration, it is more convenient to work with the stress σ_{xx} instead of u. Further, we would like to introduce the following transformations:

$$\beta=\frac{c^2 t}{2\alpha} \tag{6}$$

$$\delta=\frac{cx}{2\alpha} \tag{7}$$

$$\sigma=\sigma_{xx}/\tilde{\alpha}(3\lambda+2\mu) \tag{8}$$

The resulting transformed equations are:

$$(1+\epsilon)\frac{\partial^2 T}{\partial\beta^2}+2(1+\epsilon)\frac{\partial T}{\partial\beta}+\epsilon\left(\frac{\partial^2\sigma}{\partial\beta^2}+2\frac{\partial\sigma}{\partial\beta}\right)=\frac{\partial^2 T}{\partial\delta^2} \tag{9}$$

$$\left(\frac{c}{c_e}\right)^2\frac{\partial^2\sigma}{\partial\beta^2}=\frac{\partial^2\sigma}{\partial\delta^2}-\left(\frac{c}{c_e}\right)^2\frac{\partial^2 T}{\partial\beta^2} \tag{10}$$

where

$$\epsilon=\frac{(3\lambda+2\mu)^2\tilde{\alpha}^2 T_0\alpha}{k(\lambda+2\mu)} \tag{11}$$

ϵ is usually a small parameter, and is neglected according to the uncoupled thermal elastic theory. Here we shall limit ourselves to considering the uncoupled theory only, as a first approximation to the non-Fourier effect. Higher order approximations can be developed as a pertubation series in ϵ. The required stress boundary and initial conditions are given by:

$$\sigma(\delta,0)=\frac{\partial\sigma}{\partial\beta}(\delta,0)=0 \qquad \delta>0$$

$$\sigma(0,\beta)=\lim_{\delta\to\infty}\sigma(\delta,\beta)=0 \qquad \beta>0 \tag{12}$$

The thermal boundary and initial conditions are given by:

$$q(0,\beta)=F_0,\quad \lim_{\delta\to\infty}T(\delta,\beta)=0,\quad T(\delta,0)=0,$$

$$q(\delta,0)=0,\ \text{or}\ \frac{\partial T}{\partial\beta}(\delta,0)=0 \tag{13}$$

Equation (9), with the terms multiplied by ϵ neglected, has recently been solved by Maurer and Thompson for a constant surface flux boundary condition using the Laplace Transform method. The solution to the Laplace Transform of Eq. (9) is given by

$$\bar{T}(\delta,p)=\frac{\alpha F_0}{kc}\frac{p+2}{p}\frac{e^{-\delta(p^2+2p)^{1/2}}}{(p^2+2p)^{1/2}} \tag{14}$$

Inversion yields:

$$T(\delta,\beta)=\frac{\alpha F_0}{kc}H(\beta-\delta)\left\{e^{-\beta}I_0(\beta^2-\delta^2)^{1/2}+2\int_\delta^\beta e^{-\zeta}I_0(\zeta^2-\delta^2)^{1/2}\gamma\zeta\right\} \tag{15}$$

where H is the Heaviside unit step function.

To solve the stress equation, we let $\delta=(C_e/c)\bar{\delta}$. Taking the Laplace Transform on σ with respect to β, we get:

$$\frac{\partial^2\bar{\sigma}}{\partial\delta^2}-p^2\bar{\sigma}=\frac{\alpha F_0}{kc}(p^2+2p)^{1/2}e^{-(c_e/c)\delta(p^2+2p)^{1/2}} \tag{16}$$

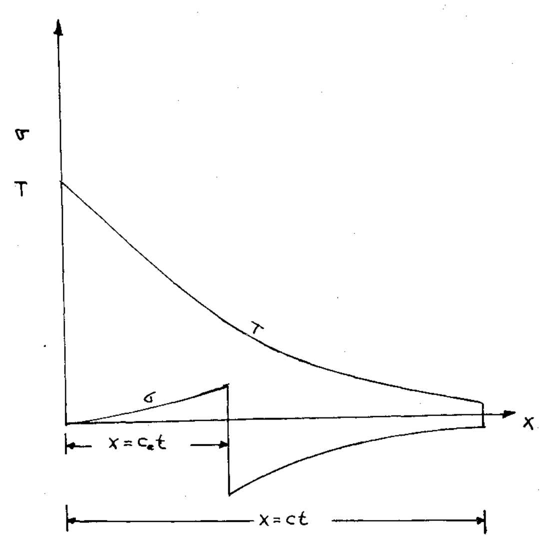

Fig. 1 Stress waves profile at time = t.

The solution for $\bar{\sigma}$ is given by:

$$\bar{\sigma}(\delta,p)=\frac{\alpha F_0}{kc}(p^2+2p)^{1/2}/[(c_e/c)^2-1]p^2+2(c_e/c)^2p]$$
$$\times\left\{e^{-(c_e/c)\delta(p^2+2p)^{1/2}}-e^{-\delta p}\right\} \quad (17)$$

Inversion yields:

$$\sigma(\beta,\delta)=-\frac{\alpha F_0}{kc}\frac{H(\beta-\delta)e^{-\beta}}{[1-(c_e/c)^2]}\{I_0(\beta^2-\delta^2)^{1/2}$$
$$+\frac{2e^{a(\beta-\delta)}}{[1-(c_e/c)^2]}\int_0^{\beta-\delta}e^{-a\eta}I_0(\eta^2+2\eta\delta)^{1/2}d\eta\}$$
$$+\frac{\alpha F_0}{kc}\frac{H(\beta-\delta)e^{-(\beta-\delta)}}{[1-(c_e/c)^2]}\{I_0(\beta-\delta)$$
$$+\frac{2e^{a(\beta-\delta)}}{[1-(c_e/c)^2]}\int_0^{\beta-\delta}e^{-a\eta}I_0(\eta)d\eta\} \quad (18)$$

where

$$a=[1+(c_e/c)^2]/[1-(c_e/c)^2]$$

Discussion of Results

Equation (18) indicates that there are 2 stress waves propagating down from the surface $x=0$, as shown pictorially in Fig. 1. The first stress wave propagates with the speed c. At the surface of this wave front $x=ct$ (or $\beta=\delta$), the stress is given by:

$$\sigma(\beta,\beta)=\frac{-\alpha F_0}{kc}\frac{1}{[1-(c_e/c)^2]}e^{-\beta}$$

This stress wave decays in the same way as the thermal wave front, and has the same magnitude as the thermal wave except by the factor of $1/[1-(c_e/c)^2]$. A second stress wave with propagation speed c_e follows. This result is in contrast to the conventional Fourier model which predicts the propagation of only one stress wave which has a speed of c_e (e.g., see Refs. 6 and 7).

As can be expected, under ordinary conditions, $c_e << c$. This 2-wave phenomenon will be significant only during a very short transient. The first wave, like the thermal wave, decays rapidly with time. It has been pointed out in Ref. 5 that the difference in the surface temperatures between the Fourier and non-Fourier model becomes less than 1 percent in about $t\sim O(50\alpha/c^2)$. However, at very low temperature, or when the order of magnitudes of c_e and c are comparable, this finite heat propagation speed cannot be ignored. The relaxation heat conduction equation must be used.

References

[1] Boley, B.A., "The Analysis of Problems of Heat Conduction and Melting," *High Temperature Structures and Materials,* Pergamon Press, New York, 1964, pp. 260-315.

[2] Peshkov, V., "Second Sound in He II," *Journal of Physics,* USSR, Vol. 8, 1944, p. 381.

[3] Chester, M., "Second Sound in Solids," *The Physical Revue,* Vol. 131, No. 5, Sept. 1963, pp. 2013-2015.

[4] Hsu, Y. Y., "On the Size Range of Active Nucleation Cavities on a Heating Surface, "*Journal of Heat Transfer,* Transactions of the ASME, Vol. 84, No. 3, Aug. 1962, pp. 207-216.

[5] Maurer, M. J. and Thompson, H. A., "Non-Fourier Effects at High Heat Flux," *Journal of Heat Transfer,* Transactions of ASME, Series C, Vol. 15, May 1973, pp. 284-286.

[6] Danilovskaya, V. Y., "Temperature Stresses in an Elastic Semi-Space Due to a Sudden Heating of its Boundary," Vol. 14, May-June 1950, pp. 316-318.

[7] Danilovskaya, V. Y., "On a Boundary Problem of Thermoelasticity," Prikladnaia Matematika i Mekhanika, Vol. 16, May-June 1952, pp. 341-344.

Wall-Wake Velocity Profile for Compressible Nonadiabatic Flows

Chen-Chih Sun* and Morris E. Childs†
University of Washington, Seattle, Wash.

Nomenclature

a = a constant in the expression $\tau=\tau_w(1-\eta^a)$ (see Ref. 5)
A = $\{[(\gamma-1)/2]\ M_e^2/(T_w/T_e)\}^{1/2}$
A_1 = $(Pr_t)^{1/2}\ \{[(\gamma-1)/2]\ M_e^2/(T_w/T_e)\}^{1/2}$
B = $\{(1+[(\gamma-1)/2]\ M_e^2/(T_w/T_e)\}-1$
B_1 = $\{(1+(Pr_t)^{1/2}\ [(\gamma-1)/2]\ M_e^2/(T_w/T_e)\}-1$
C = a constant in law of the wall (usually 5.1)
C_f = skin friction coefficient $\tau_w/(1/2)\rho_e u_e^2$
C_1 = $5.1-0.614/ak+(1/k)\ln(\delta U_\tau/\nu_w)$
K = constant in mixing length (usually 0.4)
M = Mach number
P = pressure
Pr_t = turbulent Prandtl number
T = temperature
u = velocity in streamwise direction
u^* = $(u_e/A)\arcsin\{[(2A^2u/u_e)-B]/(B^2+4A^2)^{1/2}\}$
u^{**} = $(u_e/A_1)\arcsin\{[(2A_1^2u/u_e)-B_1]/(B_1^2+4A_1{}^2)^{1/2}\}$
u_τ = friction velocity $(\tau_w/\rho_w)^{1/2}$
U^* = $u^*+(u_e/A)\arcsin\{B/(B^2+4A^2)^{1/2}\}$
W = Coles universal wake function
y = coordinate normal to wall
γ = ratio of specific heat
δ = boundary-layer thickness
δ^* = displacement thickness
Δ = $\int_0^\delta \frac{(u_e^{**}-u^{**})}{u_\tau}dy$
θ = momentum thickness
η = y/δ
ν = kinematic viscosity
Π = coefficient of wake function
ρ = density
τ = shear stress

Subscripts

e = freestream conditions
0 = stagnation conditions
w = conditions at the wall

Introduction

THE wall-wake velocity profile has been used to represent turbulent boundary-layer profiles for both adiabatic and nonadiabatic flows and for flows with or without pressure gradients.[1-5] A least squares fit of a wall-wake velocity profile to an experimental velocity profile may be used to determine C_f and δ for the profile. An accurate representation of the mean velocity distribution in the turbulent boundary layer can be very useful in integral analyses of turbulent flow problems. In the analysis of flows in which strong interactions occur (as for example in shock wave boundary-layer interactions) and in which combined viscid-inviscid analyses are required, a profile which provides a good representation of both C_f and δ can be quite important. With most earlier versions of the wall-wake profile, the velocity

Received Sept. 25, 1975; revision received March 15, 1976. This work was supported by NASA Grant NGR-48-002-047, under administration of the Aerodynamics Branch, Ames Research Center.

Index categories: Boundary Layers and Convective Heat Transfer – Turbulent; Supersonic and Hypersonic Flow.

*Research Assistant Professor, Department of Mechanical Engineering. Member AIAA.

†Professor and Chairman, Department of Mechanical Engineering. Member AIAA.